Title
Method measuring oxygen tension and transport within subcutaneous devices

Journal
Journal of Biomedical Optics, 19(8)

ISSN
1083-3668

Authors
Weidling, John
Sameni, Sara
Lakey, Jonathan RT
et al.

Publication Date
2014-08-27

DOI
10.1117/1.jbo.19.8.087006

Peer reviewed

Journal of Biomedical Optics

BiomedicalOptics.SPIEDigitalLibrary.org

Method measuring oxygen tension and transport within subcutaneous devices

John Weidling
Sara Sameni
Jonathan R. T. Lakey
Elliot Botvinick

SPIE.

Method measuring oxygen tension and transport within subcutaneous devices

John Weidling,[a,b,†] Sara Sameni,[a,b,†] Jonathan R. T. Lakey,[b,c] and Elliot Botvinick[a,b,c,d,*]
[a]University of California Irvine, Beckman Laser Institute and Medical Clinic, Irvine, California 92617, United States
[b]University of California Irvine, Department of Biomedical Engineering, Irvine, California 92617, United States
[c]University of California Irvine, Department of Surgery, Orange, California 92868, United States
[d]University of California Irvine, Edwards Lifesciences Center for Advanced Cardiovascular Technology, 1002 Health Sciences Road, Irvine, California 92617, United States

Abstract. Cellular therapies hold promise to replace the implantation of whole organs in the treatment of disease. For most cell types, *in vivo* viability depends on oxygen delivery to avoid the toxic effects of hypoxia. A promising approach is the *in situ* vascularization of implantable devices which can mediate hypoxia and improve both the lifetime and utility of implanted cells and tissues. Although mathematical models and bulk measurements of oxygenation in surrounding tissue have been used to estimate oxygenation within devices, such estimates are insufficient in determining if supplied oxygen is sufficient for the entire thickness of the implanted cells and tissues. We have developed a technique in which oxygen-sensitive microparticles (OSMs) are incorporated into the volume of subcutaneously implantable devices. Oxygen partial pressure within these devices can be measured directly *in vivo* by an optical probe placed on the skin surface. As validation, OSMs have been incorporated into alginate beads, commonly used as immunoisolation devices to encapsulate pancreatic islet cells. Alginate beads were implanted into the subcutaneous space of Sprague–Dawley rats. Oxygen transport through beads was characterized from dynamic OSM signals in response to changes in inhaled oxygen. Changes in oxygen dynamics over days demonstrate the utility of our technology. [DOI: 10.1117/1.JBO.19.8.087006]

Keywords: *in vivo* oxygen measurement; tissue transplantation; assessment of perfusion.

Paper 140348R received Jun. 3, 2014; revised manuscript received Jul. 27, 2014; accepted for publication Jul. 28, 2014; published online Aug. 27, 2014.

1 Introduction

Nonautologous tissue transplantation is a promising approach to overcome the scarcity of human pancreas donor tissue in the treatment of type 1 diabetes.[1–5] To this end, we have developed a scalable islet of Langerhans (islet) isolation method wherein partially digested piglet pancreatic tissue is matured *in vitro* over 8 days by incubation in a novel cell culture media.[6,7] During this period, exocrine tissue dies and isolated islets remain, which we have shown to be responsive to glucose challenges. Isolated islets can be encapsulated within permeable hydrogels such as alginate to provide an immunoprotective barrier that may preclude pharmacological immunosuppression.[8,9] However, encapsulation devices introduce a transport barrier between the host and graft tissues and inherently limit oxygen supply, compromising graft function and cell viability,[10] problems that scale with device wall thickness.[11,12]

Typically grafts are implanted in subcutaneous[13] or intraperitoneal[14] sites where partial pressures of oxygen (pO_2) are approximately 60 and 40 mm Hg, respectively, which is lower than that of arterial blood (>80 mm Hg). It is commonly asserted that low cell viability within devices[15,16] results from low tissue oxygen taken together with device diffusional barriers to create hypoxic and anoxic conditions, where these conditions are known to promote cell death through necrosis and apoptosis.[17] However, direct measurement of oxygen levels within microencapsulated devices *in vivo* has not been previously reported, where such measurements are ultimately required to assay the efficacy of implant technologies that claim to promote oxygen delivery. In a study of relatively large alginate disc implants (1 to 1.5 cm^2 surface area at 3- to 6-mm thick) by Veriter et al.,[18] oxygen within implanted devices was directly measured through the use of electronic paramagnetic resonance oximetry in rats. However, current research shows that such thick devices cannot retain islet function, likely due to diffusional limitations, thus promoting microencapsulation technologies such as thin sheets or microbeads of permeable materials.

We have developed a technology for the direct measurement of oxygen partial pressures within such implanted devices. Our technology comprises oxygen-sensitive microparticles (OSMs) and an electro-optical probe to noninvasively excite OSMs and record emitted light from which pO_2 is determined. Additionally, we have developed a protocol to measure both the steady state pO_2 within devices as well as transport dynamics between the device and the local vasculature. This is especially important for pancreatic islets transplantation because islets are metabolically demanding and are sensitive to decreases in tissue oxygenation. Although native islets contain an extensive capillary network,[19] implanted devices typically do not, and are limited in their ability to supply oxygen to encapsulated pancreatic islets.[10] Consequently, these islets are subject to hypoxic or anoxic conditions,[15,16] contributing to the death of 40% of pancreatic islets in implants after just 4 weeks.[20] Strategies

*Address all correspondence to: Elliot Botvinick, E-mail: elliot.botvinick@uci.edu

†These authors contributed equally to this work.

aimed at improving oxygenation within biomaterial-encapsulated islets should significantly improve the chances of a successful transplant.[21] These strategies can be tested with our technology to rule out approaches that do not mitigate a period of hypoxia post transplantation.

2 Method for Preparing Alginate Beads Containing Oxygen Sensing Microparticles

2.1 *Preparation of OSMs*

OSMs are made from an oxygen-sensitive dye embedded within a polystyrene matrix. Two types of OSMs were fabricated, each comprising a unique oxygen-sensing metalloporphyrin dye. The first is platinum(II) meso-tetraphenyl tetrabenzoporphine (PtTPTBP, Frontier Scientific, Logan) and the second is platinum(II) meso-tetra(pentafluorophenyl)porphine (PtTFPP, Frontier Scientific, Logan). OSMs are fabricated by first mixing 2 mg of dye with 30 mg of polystyrene (M_w 2500, Sigma, St. Louis) and then dissolving the mixture in 450 μl of chloroform (Sigma). The solution is pipetted and spread onto a glass slide to polymerize overnight in room air at 23°C. The resulting thin film is scraped off with a razor blade and crushed into small micron-sized particles using a glass mortar and pestle.

2.2 *Encapsulation of OSMs Within Alginate Beads*

Clinical grade ultrapure low viscosity alginate (UPLVM, Novamatrix, Sandvika, Norway) is dissolved in deionized water at 3 wt. % and sterile filtered using a 0.22 μm syringe filter. OSMs are suspended in 1.5 mL of the UPLVM solution and loaded into an encapsulator (Nisco, Zurich, Switzerland) for the fabrication of alginate beads. Specifically, the solution is first loaded into a syringe and then driven through a 25 G needle under positive gas pressure (4 PSI, N_2). The needle is held at 9 V relative to a 120 mM $CaCl_2$ solution within a Petri dish placed below the tip of the needle. Alginate beads form at the tip of the needle and fall into the $CaCl_2$ solution for alginate polymerization. A typical OSM alginate bead is shown in Fig. 1. Bead size is dependent on gas pressure, voltage, and the distance between the needle and media in the dish. For these experiments, the average diameter of alginate beads was found to be 415 ± 47.68 μm.

3 Probing pO_2 Within Alginate Beads

3.1 *Optical Probe for In Vitro Experiments*

An optical probe was constructed to simultaneously measure both OSM types (Fig. 2). The two OSM types are spectrally separated. PtTFPP OSMs have multiple absorption peaks at 390, 504, and 538 nm and emission peaks at 647 and 710 nm.[22] PtTPTBP OSMs have multiple absorption peaks at 430 and 614 nm and an emission peak at 770 nm.[22] The optical probe can selectively excite either type of OSM with two pairs of light emitting diode (LEDs) (Rebel LED, Luxeon Star, Brantford, Canada) centered at 530 nm (green) and 617 nm (red) for PtTFPP and PtTPTBP, respectively. The LEDs are mounted onto a custom three-dimensional printed conical mount designed to pitch the LEDs such that emitted light converges onto samples placed just above the surface of the cone. The conical mount is glued onto the distal surface of a 2-in. long lens tube (Thorlabs, Newton) containing a 6.4-mm diameter image conduit (Edmund Optics, Barrington) and a focusing lens ($f = 25$ mm). The distal end of the lens tube is mounted onto a filter cube holder (Thorlabs) containing a long-pass dichroic beam splitter (FF740-Di01, Semrock, Rochester) to reflect PtTFPP and transmit PtTPTBP emissions, respectively. Two amplified photodiode detectors (PDA100A, 9.8-mm diameter, Gain = 30, Thorlabs) are mounted onto the cube to detect emissions from each OSM type. LED emission and digitalization of photodiode signals are conducted by a National Instruments data acquisition device (USB6361 DAQ, National Instruments, Austin) controlled by LabView (National Instruments).

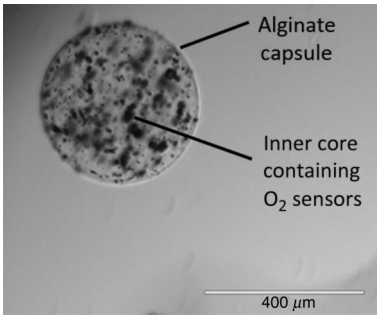

Fig. 1. An alginate capsule containing oxygen-sensitive microparticle (OSM) sensors.

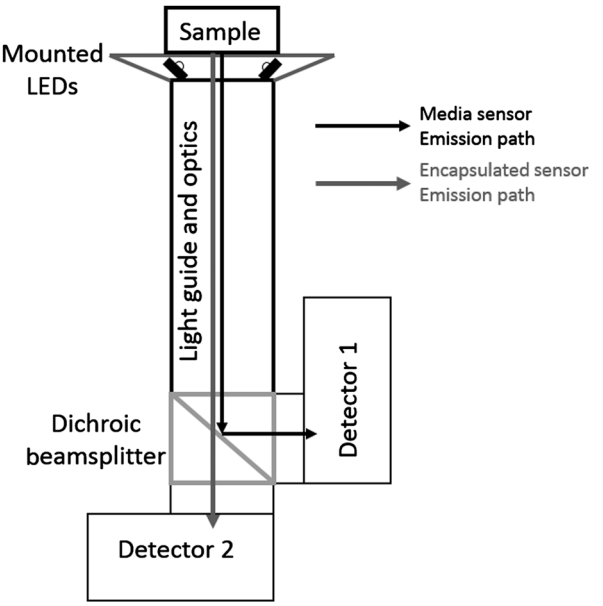

Fig. 2 Illustration of optical probe used for *in vitro* measurement. Emitted light from the two OSM types is separated spectrally onto two separate detectors.

3.2 *Determining Oxygen Partial Pressure From OSM Emission*

OSMs were calibrated from measurements acquired at different pO_2 levels, as provided by four gas tanks containing different oxygen mixtures. OSM emission was analyzed using the method of luminescence lifetime. OSMs were optically excited by pulsing LEDs in a 100 Hz square-wave with a 50% duty cycle. Optical signals were sampled at 1 MHz. OSMs were probed every 20 s, where at each time point, 25 measurements were acquired at 100 Hz and averaged. The metalloporphyrin dye within OSMs continues to emit light after the cessation of each LED light pulse. This emission is modeled as an exponential decay as

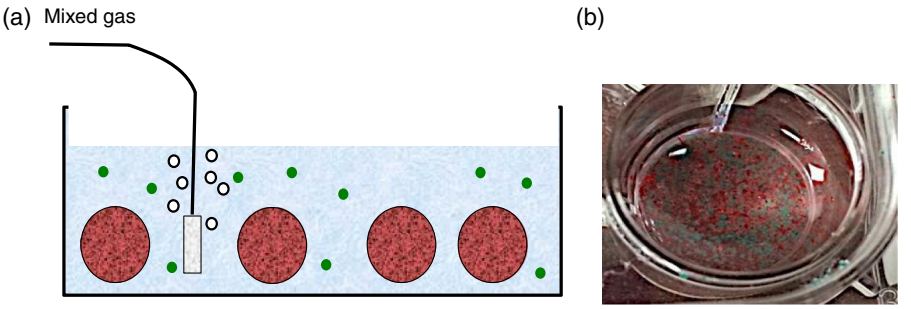

Fig. 3 (a) *In vitro* test system. Two spectrally distinct OSM types are suspended in a PBS bath within a well: one to monitor the PBS (green circles) and one to monitor the alginate capsules (red circles). (b) Close up view showing PBS and encapsulated OSMs within a well.

$$V(t) = V_0 e^{\left(\frac{-t}{\text{Tau}}\right)}, \quad (1)$$

where V is the detector voltage, V_0 is the voltage at the start of the decay, t is the time, and Tau is the lifetime decay time constant. Dye emission is quenched by oxygen and consequently, Tau decreases with increasing pO_2. The relationship between pO_2 and Tau is described by a modified Stern–Volmer relationship[23]

$$\frac{\text{Tau}}{\text{Tau}_0} = \frac{f}{1 + K_{SV}[O_2]} + 1 - f, \quad (2)$$

where Tau is the oxygen-dependent lifetime decay time constant, Tau_0 is the zero oxygen lifetime decay constant, f is the fraction of emission of one site of a two-site model,[24] and K_{SV} is the Stern Volmer constant. K_{SV} and f were estimated by optimization.

3.3 *In Vitro Measurement of Oxygen Partial Pressure Within Alginate Beads*

Alginate beads containing PtTPTBP OSMs and unencapsulated PtTFPP OSMs were suspended in 1 mL of media phosphate buffered saline (PBS) within a single well of a 24-well dish (Corning Inc., Corning) in which gas was bubbled (Fig. 3) with either compressed air (21% oxygen), or precalibrated mixtures of 10% oxygen/90% nitrogen, 5% oxygen/95% nitrogen, or argon gas (0% oxygen).

Figure 4 plots pO_2 as reported by both the encapsulated and nonencapsulated OSMs versus time for a series of gas exchanges. The pO_2 levels were calculated by first computing the mean steady state lifetime values for each gas concentration using Eq. (1). Regression of lifetime against gas concentration as computed by Eq. (2) ($R^2 > 0.99$) provides a calibration equation mapping lifetime to pO_2. Data confirms oxygen sensitivity within the alginate bead and no significant dynamic delay between the PBS and the volume of the bead (Fig. 4).

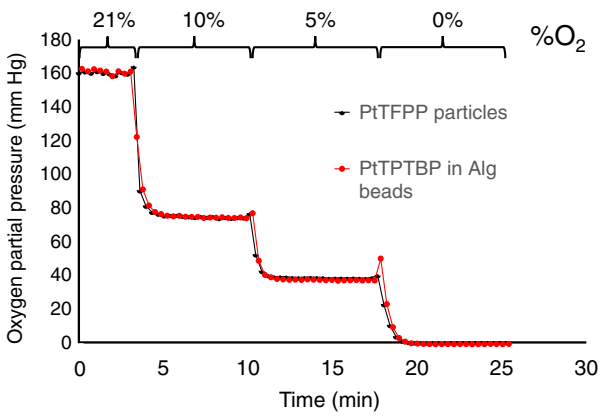

Fig. 4 *In vitro* measurements. pO_2 for a set of gases containing oxygen at 21%, 10%, 5%, and 0%. Black line: pO_2 in PBS and red line: pO_2 in alginate capsules.

4 Measuring pO_2 and Transport Dynamics *In Vivo*

4.1 *In Vivo Probe*

A compact *in vivo* optical probe was constructed for PtTPTBP OSMs alone [Fig. 5(a)]. Since only one dye is being measured *in vivo* there is no need for the more complex optical setup used in the *in vitro* experiment. Two of the 617-nm centered LEDs were mounted on the conical mount, as described above. The conical mount was then placed directly on the photodiode module and aligned with the active area of the photodiode. A 715 nm high-pass optical filter (Semrock) is mounted above the surface of the photodiode. The conical mount is placed directly onto the skin during measurements.

4.2 *In Vivo* pO_2

In vivo testing was performed to determine if PtTPTBP OSM signals can be related to pO_2 within subcutaneously implanted alginate beads. A small incision was made on the anterior side of an anesthetized rat (Sprague–Dawley, Charles River Laboratories, Wilmington). Anesthesia was maintained with a gas mixture of 100% oxygen and vaporized isoflurane delivered to a nose cone placed over the snout. OSM-containing beads were then implanted subcutaneously via pipette injection in a small pocket formed in the subcutaneous space by blunt dissection. The incision was closed using a wound sealing adhesive

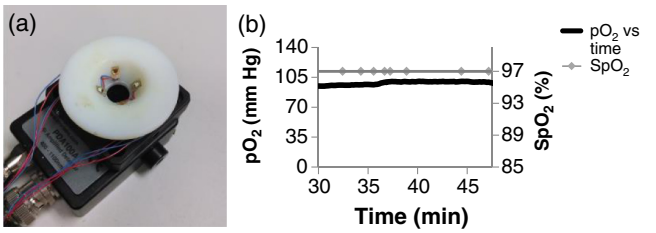

Fig. 5 *In vivo* measurements. (a) Optical probe used for *in vivo* measurements. (b) Day 5 pO_2 and SpO_2. Animals were anesthetized during measurements with a mixture of isoflurane and 100% oxygen.

(Gluture, Abbott, Abbott Park). pO_2 within beads was then optically probed on demand through the skin. Rats were fixed with a rodent pulse oximeter (Kent Scientific, Torrington) placed on the front paw to simultaneously measure oxygen saturation of blood hemoglobin (SpO_2) and heart rate.

Figure 5(b) shows pO_2 data acquired on day 5 post implantation during anesthesia. As expected, SpO_2 was constant at normal physiological levels (95% to 100%) and pO_2 within the beads was ~100 mm Hg, indicating gas exchange both through the vasculature and skin.

The data collected *in vivo* was analyzed for its accuracy. Decay curves were collected as described above (measurements taken every 10 s with 25 curves for each measurement). After averaging the 25 curves, the variance at each point was found to be <0.5% of the mean value [Eq. (1)]. In the absence of OSMs, the detector returns an exponential decay of Tau ~15 μs. To determine the weight of this effect on OSM-mediated signals, the mean signal value between 0 and 50 μs of OSM-mediated signals was divided by that for the OSM-free signals. The ratio was >7, which we found was insignificant for fitting OSM lifetimes.

4.3 *Variable Inhaled Gas Experiment*

We developed an assay to measure transport dynamics between the microbeads and local vasculature. Such an assay is important since it captures effects of both increase/decrease of local vasculature resulting from the implantation wound and subsequent healing as well as the deposition of new collagenous tissue, which forms an additional diffusional barrier. Inhaled gas is rapidly changed as pO_2 and SpO_2 are monitored. Oxygen dynamics after each gas change are governed by tissue architecture, with rise/fall times increasing or decreasing as the local tissue rejects or perfuses the implant, respectively.

For these tests, the 100% oxygen + isoflurane inhaled gas was transiently exchanged with room air (21% oxygen) + isoflurane and then returned to 100% oxygen + isoflurane. OSMs were probed every 10 s. Measurements were recorded on days 5 and 9 post implantation.

Figure 6(a) shows a typical variable inhaled gas experiment at day 5. pO_2 and SpO_2 exhibited dynamics in the early stages of anesthesia (first 30 min) and eventually reached a steady state when breathing the 100% gas mixture. This phenomenon was common to most of our experiments and is likely due to the physiological effects of isoflurane. The gas was changed to the room air mixture for ~10 min and then returned to the 100% O_2 mixture for ~25 min. pO_2 within beads did not reach a steady state within the 10 min of room air, but did within the 25 min of 100% O_2. Similar results were observed for the second room air challenge beginning at ~72 min.

The variable inhaled gas experiment was repeated for the same rat on day 9 [Fig. 6(b)]. Here, pO_2 reaches a steady state within the ~10 min of room air gas indicating rapid O_2 exchange between the beads and tissues as compared to day 5, an effect most likely mediated by tissue remodeling.

5 Conclusions and Future Directions

One of the great challenges for creating a successful nonautologous cellular therapy is to provide the new cells in the body with sufficient oxygen and nutrient transfer to survive while protecting them from the immune system. An array of techniques for encapsulating islet cells in alginate has been studied and tested extensively, but ultimately fail within weeks due to, in part, hypoxic conditions. We have developed a technique for measuring the oxygen concentration continuously inside an implanted object, such as an alginate bead, and verified its operation *in vivo* in rats by measuring its response to changing inhaled oxygen concentrations and comparing that response at two time points within the first week of implantation, during which wound healing is most active. The results showed that our technique tracks changes in oxygen in implanted alginate beads and that the rate of oxygen transfer to the implanted beads increased during the wound healing process. This link between wound healing and oxygen transport dynamics within the implanted microbeads could have implications for identifying designs that lead to either cell survival or cell death. By knowing the amount of oxygen inside the implants, one may be able to correlate that level with critical points in the wound healing process, such as new vessel formation or the identification of areas that have become "walled-off" from the body.

Optical oxygen sensing using luminescent dyes has gained popularity and is used in some commercial fiber-based optical oxygen probes, such as the Ocean Optics NeoFox system, and the PreSens oxygen probes (which can be used in biological applications). These devices show that the luminescence-based sensing of oxygen is reliable, but they fall short of being able to measure within implanted materials on small scales and would require a tethered component crossing the skin surface. Other technologies exist to noninvasively measure oxygen levels proximal to an implant, but these technologies do not

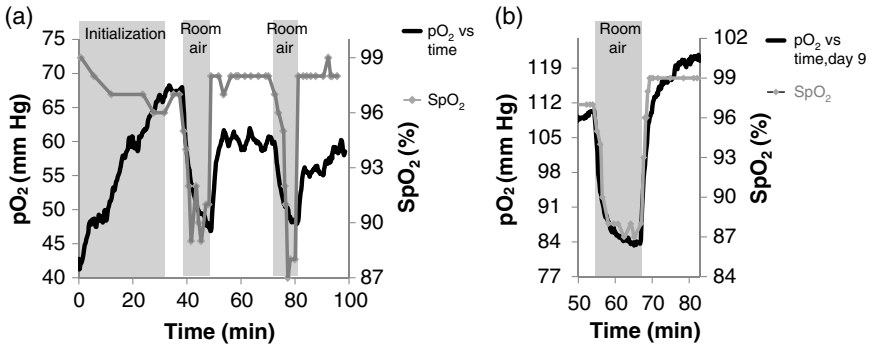

Fig. 6 (a) Variable inhaled gas experiment. On day 5, SpO_2 and pO_2 within capsules consistently exhibit dynamics after the initiation of anesthesia, stabilizing after approximately 30 min. At 37 min, the percent oxygen mixed with isoflurane was changed from 100% to 21% for 11 min and then switched back. The same exchange in inhaled gas is repeated 26 min later. (b) On day 9, pO_2 within capsules exhibits faster dynamics following a gas exchange as compared to day 5.

measure oxygen within the device and thus cannot report on the microenvironment of encapsulated tissues. Such technologies include oxygen electrodes either implanted or in contact with skin,[25,26] or scattered light methods such as diffuse optical spectroscopy (SpO_2 measurement). Our technology has been demonstrated to continuously measure pO_2 within implanted alginate microbeads using inexpensive optical components coupled to a standard data acquisition device. Microbead pO_2 values measured subcutaneously in our study (~45 to 120 mm Hg) were higher than those reported by Veriter et al. (~5 to 40 mm Hg) where larger alginate devices were implanted in a similar manner. This difference can be attributed to differential tissue responses or the accuracy of the sensor. Our calibration against known gases had a regression coefficient of $R^2 > 0.99$ indicating the accuracy of our system, and we have found that alginate microbeads elicit a moderate tissue response as compared to a slab (unpublished data). Future studies are planned to encapsulate islets along with OSMs and correlate pO_2 with implant functionality and cell survival. This will provide quantitative evidence concerning the role of oxygen transport in reported failed approaches to islet encapsulation for reversal of type 1 diabetes. Additionally, our technique can evaluate new encapsulation technologies for their oxygen transport characteristics.

Acknowledgments

The authors would like to acknowledge Michael Alexander for providing training on animal procedures and providing technical support during animal procedures. E. Botvinick acknowledges the Air Force Office of Scientific Research (FA9550-10-1-0538) and the National Institutes of Health (P41EB015890). J. Lakey acknowledges financial and institutional support from Department of Surgery, University of California Irvine.

References

1. C. D. Ching et al., "A reliable method for isolation of viable porcine islets," *Arch. Surg.* **136**(3), 276–279 (2001).
2. C. G. Thanos and R. B. Elliot, "Encapsulated porcine islet transplantation: an evolving therapy for the treatment of type I diabetes," *Expert Opin. Biol. Ther.* **9**(1), 29–44 (2009).
3. D. Sutherland et al., "Isolation of human and porcine islets of Langerhans and islet transplantation in pigs," *J. Surg. Res.* **16**(2), 102–111 (1974).
4. M. Larsen and B. Rolin, "Use of the Gottingen Minipig as a model of diabetes, with special focus on type 1 diabetes research," *ILAR J.* **45**(3), 903–313 (2004).
5. G. S. Korbutt et al., "Neonatal porcine islets as a possible source of tissue for humans and microencapsulation improves the metabolic response of islet graft post transplantation," *Ann. N. Y. Acad. Sci.* **831**(1), 294–903 (1997).
6. M. Lamb et al., "In vitro maturation of viable islets from partially digested young pig pancreas," *Cell Transplant.* **23**(3), 263–272 (2013).
7. C. Kuehn et al., "Young porcine endocrine pancreatic islets cultured in fibrin show improved resistance toward hydrogen peroxide," *Islets* **5**(5), 0–7 (2013).
8. M. D. Darrabie et al., "Characteristics of poly-l-ornithine-coated alginate microcapsules," *Biomaterials* **26**(34), 6846–6852 (2005).
9. P. de Vos et al., "Multi scale requirements for bioencapsulation in medicine and biotechnology," *Biomaterials* **30**(13), 2559–2570 (2009).
10. J. Schrezenmeir et al., "Long-term function of porcine islets and single cells embedded in barium-alginate matrix," *Horm. Metab. Res.* **25**(4), 204–209 (1993).
11. K. Chowdary, K. P. Mohapatra, and M. Krishna, "Evaluation of olibanum resin as a new microencapsulating agent for aceclofenac controlled release microcapsules," *Indian J. Pharm. Sci.* **68**(4), 461–464 (2006).
12. K. Fehsel et al., "Necrosis is the predominant type of islet cell death during development of insulin-dependent diabetes mellitus in BB rats," *Lab. Invest.* **83**(4), 549–559 (2003).
13. N. Chang et al., "Direct measurement of wound and tissue oxygen tension in postoperative patients," *Ann. Surg.* **197**(4), 470–478 (1983).
14. R. B. Spokane et al., "An implanted peritoneal oxygen tonometer that can be calibrated in situ," *ASAIO Trans.* **36**(3), M719–M722 (1990).
15. J. Schrenzenmeir et al., "Effect of microencapsulation on oxygen distribution in islet organs," *Transplantation* **57**(9), 1308–1314 (1994).
16. J. Schrezenmeir et al., "The role of oxygen supply in islet transplantation," *Transplant. Proc.* **24**(6), 2925–2929 (1992).
17. C. Michiels, "Physiological and pathological responses to hypoxia," *Am. J. Pathol.* **64**(6), 1875–1882 (2004).
18. S. Veriter et al., "In vivo selection of biocompatible alginates for islet encapsulation and subcutaneous transplantation," *Tissue Eng. Part A* **16**(5), 1503–1513 (2010).
19. S. Bonner-Weir, "Morphological evidence for pancreatic polarity of β-cell within islets of Langerhans," *Diabetes* **37**(5), 616–621 (1988).
20. P. De Vos et al, "Why do microencapsulated islet grafts fail in the absence of fibrotic overgrowth?," *Diabetes* **48**(7), 1381–1388 (1999).
21. J. Schrezenmeir et al., "Immobilized hemoglobin improves islet function and viability in the bioartificial pancreas in vitro and in vivo," *Transplant. Proc.* **26**(2), 792–800 (1994).
22. M. Quaranta, S. M. Borisov, and I. Klimant, "Indicators for optical oxygen sensors," *Bioanal. Rev.* **4**(2–4), 115–157 (2012).
23. S. M. Borisov et al., "Phosphorescent platinum (II) and palladium (II) complexes with azatetrabenzoporphyrins—new red laser diode-compatible indicators for optical oxygen sensing," *ACS Appl. Mater. Interfaces* **2**(2), 366–374 (2010).
24. E. R. Carraway et al., "Photophysics and photochemistry of oxygen sensors based on luminescent transition-metal complexes," *Anal. Chem.* **63**, 337–342 (1991).
25. R. Ladurner et al., "Predictive value of routine transcutaneous tissue oxygen tension ($tcpO_2$) measurement for the risk of non-healing and amputation in diabetic foot ulcer patients with non-palpable pedal pulses," *Med. Sci. Monit.* **16**(6), 273–277 (2010).
26. D. De Backer et al., "Monitoring the microcirculation in the critically ill patient: current methods and future approaches," *Appl. Physiol. Intensive Care Med.* **2**, 263–275 (2012).

John Weidling is a PhD student in the Department of Biomedical Engineering at the University of California, Irvine, United States. He is training in the laboratory of Elliot Botvinick. His dissertation work is the invention and development of a continuous lactate monitor for human health.

Sara Sameni is a PhD student in the Department of Biomedical Engineering at the University of California, Irvine, United States. She is training in the laboratories of Elliot Botvinick and Jonathan Lakey. Her dissertation work is the investigation of new technologies for xenotransplantation of pancreatic tissue in the treatment of type 1 diabetes.

Jonathan R. T. Lakey received his PhD degree in experimental surgery from the University of Alberta, Edmonton, Canada. He is an associate professor of surgery and biomedical engineering at the University of California, Irvine, United States. He is a director of the Clinical Islet Program and director of research in the Department of Surgery. He has research laboratories in the Department of Surgery and the Sue and Bill Gross Stem Cell Institute. He works in the areas of diabetes, islet transplantation, and stem cell biology.

Elliot Botvinick received his PhD degree in bioengineering from University of California, San Diego, United States. He is an associate professor of biomedical engineering and surgery at the University of California, Irvine, United States. He has research laboratories in the Beckman Laser Institute and the Edwards Lifesciences Center for Advanced Cardiovascular Technology. He works in the areas of mechano-biology, mechano-transduction, and tissue engineering.